Cretaceous Research 62 (2016) 98–108

Contents lists available at ScienceDirect

Cretaceous Research

journal homepage: www.elsevier.com/locate/CretRes

Aptian giant explosive volcanic eruptions in the Songliao Basin and northeast Asia: A possible cause for global climate change and OAE-1a

Pujun Wang*, Chongyang Chen, Haibo Liu

College of Earth Sciences, Jilin University, Changchun 130061, PR China

ARTICLE INFO

Article history:
Received 14 May 2015
Received in revised form
4 September 2015
Accepted in revised form 26 September 2015
Available online 9 October 2015

Keywords:
Cretaceous Songliao Basin
Aptian volcanism in NE Asia
Volcanic ash aerosol greenhouse gases
Climate changes and OAE-1a
Isotope excursion

ABSTRACT

Volcanism is a natural climate force that causes variations in temperatures. The Aptian Oceanic Anoxic Event 1a (OAE-1a) was preceded by a prominent negative C-isotope excursion attributed to major volcanism of the Ontong Java plateau (OJP), which presumably resulted in a pCO_2 increase and a climatic change. However, the OJP alone may not adequately explain some important isotopic signatures such as the negative strontium-isotope excursion from 125 Ma to 113 Ma that is recorded in the corresponding marine deposits. We present an independent and hitherto undocumented case, the giant Aptian volcanism in the Songliao Basin and northeast Asia (SB-V) on the Cretaceous active continental margin between the Eurasian and the Pacific plates, which covered an area of ca. 2.3×10^6 km^2, nearly matching the simultaneous case of the OJP. Intensive strong, explosive volcanic eruptions of the SB-V occurred at 121–109 Ma and introduced a large volume of fine-grained volcanic ash and degassing volatiles into the atmosphere. The Aptian isotopic ratios ($^{87}Sr/^{86}Sr$, $^{206}Pb/^{204}Pb$, $^{207}Pb/^{204}Pb$, and $^{208}Pb/^{204}Pb$) of marine carbonates from the Mid-Pacific shift in values between their Barremian pre-excursion high values and the negative magmatic values of the SB-V. The transient global cooling at the onset of the OAE-1a coincided with the beginning of the violent acidic eruption of the SB-V (119.9–120.2 Ma). We therefore infer that the SB-V must have played a role in the Aptian global climatic changes and OAE-1a through the heavy fall of volcanic dust and the outgassing of aerosol and greenhouse gases.

1. Introduction

Several important global geological events occurred during the Aptian, including the Oceanic Anoxic Event 1a (OAE-1a, ~120 Ma) and various climatic changes (Zakharov et al., 2013). The OAE-1a is characterized by quasi-global deposition of organic-rich black shale (Misumi, Yamanaka, & Tajika, 2009). Climatic warming resulted from a prominent increase of CO_2 concentrations in the atmosphere (Föllmi, 2012). Notable contemporaneous changes in various stable isotopes of marine deposits have been recognized both in the Tethys and Pacific Oceans (van Breugel et al., 2007). Modern observations have confirmed that volcanic eruptions are an important natural cause of climate change at many time scales (Robock, 2000; Sigl et al., 2013). Cretaceous volcanic activities, including large igneous provinces (LIPs) and continental flood basalt provinces (CFBPs), also showed a causal relationship with the paleo-greenhouse climate (Keller, 2008; Wang et al., 2014).

The Ontong Java Plateau (OJP), which was an Aptian giant flood basalt event in the Mid-Pacific, was considered to be the major cause for the OAE-1a and corresponding climatic warming (Keller et al., 2011). However, the OJP alone cannot explain some key facts concerning the geochemical signatures recorded in the Aptian marine deposits. For example, the $^{87}Sr/^{86}Sr$ in marine deposits showed a generally continuous negative trend throughout the entire Aptian from 121 Ma to 113 Ma (Jenkyns & Wilson, 1999). This is contradictory to the genetic explanation regarding an isotopic shift mainly caused by OJP volcanism because the OJP appears to have been formed rapidly at approximately 120 Ma (Fitton, Mahoney, Wallace, & Saunders, 2004), while the negative excursion of $^{87}Sr/^{86}Sr$ recorded in the marine deposits climaxed at approximately 113 Ma (Jenkyns & Wilson, 1999), which was much later than the OJP event. In addition, after the OAE-1a, the OJP became quiescent and the strontium-87 radioactive source from continental weathering increased, both of which could have had caused a positive excursion of the strontium isotope relative to the intensive OJP episode either in marine water or in sediments

* Corresponding author. 2199 Jianshe Street, College of Earth Sciences, Jilin University, Changchun 130061, PR China.
E-mail address: wangpj@jlu.edu.cn (P. Wang).

http://dx.doi.org/10.1016/j.cretres.2015.09.021
0195-6671/

according to the geological principle $^{87}Sr/^{86}Sr$ ratios (Larson & Erba, 1999). There was also an inconsistency between isotopes of lead and osmium recorded in the Aptian marine deposits when only the OJP was considered. $^{187}Os/^{188}Os$ records from the Mid-Pacific Mountains and the Alps of northern Italy showed similar trends, although they were very distant from each other in the Early Cretaceous. This has been explained by very efficient ocean mixing and elevated rates of silicate weathering on the continents due to global warming during the OAE-1a (Bottini, Cohen, Erba, Jenkyns, & Coe, 2012). However, the Pb isotopic compositions from the Pacific and Italy showed very different features. The Pb isotopic composition from the Pacific showed rapid fluctuations between unradiogenic and radiogenic values, while Pb isotopic composition from Italy remained unchanged, with values mostly identical to those of the upper continental crust. Thus, a limited dispersion of Pb-carrying particles out of the Pacific Ocean was proposed to explain the lead isotope record (Kuroda et al., 2011). To explain the isotope excursion problems discussed above, we proposed a new model that attributes the isotopic signatures of the Aptian marine deposits to a possible impact of the giant Aptian volcanism in the Songliao Basin and northeast Asia (SB-V) through the fallout of wind-driven volcanic ash.

Other geological events independent from the OJP volcanism should be considered in relation to the OAE-1a and the global climatic changes in the Aptian. Large-scale volcanic phases have been recognized in the Songliao Basin and the entire region of northeast Asia, which were located on the active continental margin of the Eurasian plate during the mid-Cretaceous (Wang, Xie, et al., 2007; Wang et al., 2015). The strongest explosive acidic volcanic eruptions occurred between 121 and 109 Ma, and the predominant eruption types were Plinian and phreatomagmatic, which had generated large volumes of fine-grained volcanic ash into the atmosphere (Figs. 1–4). The fine volcanic dust had reasonably provided a magmatic origin for the negative isotopes of strontium and lead, which may have significantly contributed to the marine sediments, especially those adjacent to northeast Asia. We further concluded that the SB-V could be a possible cause for global climate change and OAE-1a through the heavy fall of volcanic dust and the outgassing of aerosol and greenhouse gases.

2. Geological background

Lower Cretaceous volcanic rocks were recognized and mapped over widespread areas in northeast Asia, both on the continent and in the adjacent oceanic crust (Petrov, Leonov, & Pospelov, 2014; Ren, Niu, Wang, Jin, & Xie, 2013). These volcanic associations have experienced regional differential subsidence since the Late Cretaceous, which resulted in mountain building, basin filling, and fault-block tilting (Ren, Tamaki, Lia, & Zhang, 2002). Although the present landforms in the region include lowlands, highlands, and mountain ranges, both volcanic and sedimentary successions formed within all of these morphologic elements, even on the present Great Xing'an mountain range, in the Aptian and Albian. The middle and lower parts of the basin fills over the entire region are typically composed of Lower Cretaceous volcanogenic successions. The distribution patterns of the volcanic successions have been identified as a result of both petroleum exploration and geological surveys (e.g., DPGC, 1993; IGS, 1991; Khanchuk, 2012).

The Songliao Basin (SB) is the largest sedimentary basin in northeast Asia, with a presently preserved area of 2.6×10^5 km^2 (Fig. 1). The SB has had an annual crude oil production of approximately one-half million tons (ca. 3.5 million barrels) and thus has received considerable attention since the late 1950s. The Aptian to lower Albian volcanic rocks, called the Yingcheng Formation (Y-Fm.) locally, have become major types of petroleum reservoirs in the SB exploration since late 1990's (Feng et al., 2011). More than 500 wells have been drilled, and high-quality 3-D seismic data are available for the buried volcanoes in the SB. Petrological, geochemical, and radiogenic isotope studies for the volcanogenic successions have been thoroughly conducted in the past 15 years (e.g., Wang, Liu, Wang, & Song, 2002; Wang, Ren, et al., 2002; Wang, Chen, Chen, Siebel, & Satir, 2006). These studies provide us with reliable constraints on the time and space distributions of the volcanic rocks (Figs. 1 and 2).

Although much work has been conducted on the Lower Cretaceous volcanic rocks in the Songliao Basin and northeast Asia (SB-V), the possible relationship between the SB-V volcanism and the Aptian global climatic event has hitherto been undocumented.

3. Materials, methods, and results

The Aptian–Albian volcanic rocks within and around the SB were the primary focus in this paper. New data on the volcanic rocks were obtained by field observation, subsurface geological mapping, and chemical analysis of bulk compositions (178 samples), isotopes of Rb–Sr (14 samples) and Pb–Pb (24 samples), and zircon U–Pb dating (8 samples). Major elements were analyzed with an X-ray fluorescence spectrometer (PW1404/10) at the analytical center of Jilin University, Changchun, China. Whole-rock Rb–Sr and Pb–Pb isotopic composition was measured on a Finnigan MAT-262 mass spectrometer at the Laboratory of Radiogenic Isotope Geochemistry, University of Science and Technology of China, Hefei, China. Details on the analytical techniques were provided by Chen, Hegner, and Todt (2000). Individual zircon crystals were used for zircon U–Pb dating, which was performed using SHRIMP II at Beijing SHRIMP Center, Institute of Geology, CAGS, Beijing and LA-ICP-MS at the State Key Laboratory of Geological Processes and Mineral Resources, China University of Geosciences, Wuhan, China. The analytical procedure of SHRIMP and LA-ICP-MS is the same as that described by Williams (1998) and Yuan et al. (2004), respectively.

The lithofacies and thickness of buried volcanoes in the SB were mapped (Fig. 1) using seismic data, well logs, drill cores, and cuttings data that were obtained during exploration of the SB. The characteristics and recognition of proximal, medial, and distal facies associations were described in detail by Wang and Chen (2015, in Table 3). In addition, 53,001 m of volcanogenic succession from 167 representative boreholes was used for lithology and facies study. Lithologic definitions are based on LeMaitre (1989). The corresponding results are shown in Fig. 3. The eruption styles of the SB-V were studied on outcrops, focusing on their structure, texture, and the assemblages of the volcanic ejecta (Fig. 4).

The statistical data used in the paper are based on both our own work on volcanic radiometric dating (such as Fig. 5) and the published literature (see data source of Table 1), the bulk composition of primary fluid inclusions hosted in the volcanic rocks (see description of Table 2), and the regional geology and stratigraphy of northeast Asia (see Table 3 and figure caption of Fig. 6). The regional stratigraphic correlations shown in Table 3 and Fig. 6 are mainly based on the radioisotopic ages of the corresponding volcanogenic successions. We have assigned two isotopic ages for each stratigraphic column at its upper and lower parts (Fig. 6①–⑦). They are mostly the Aptian to lower Albian successions.

4. Aptian–Albian volcanism in the Songliao Basin (Yingcheng Formation)

The Yingcheng Formation volcanic successions (Y-Fm.) experienced two episodes of eruption during the Aptian and Albian. The first episode is characterized by large-scale rhyolitic explosive

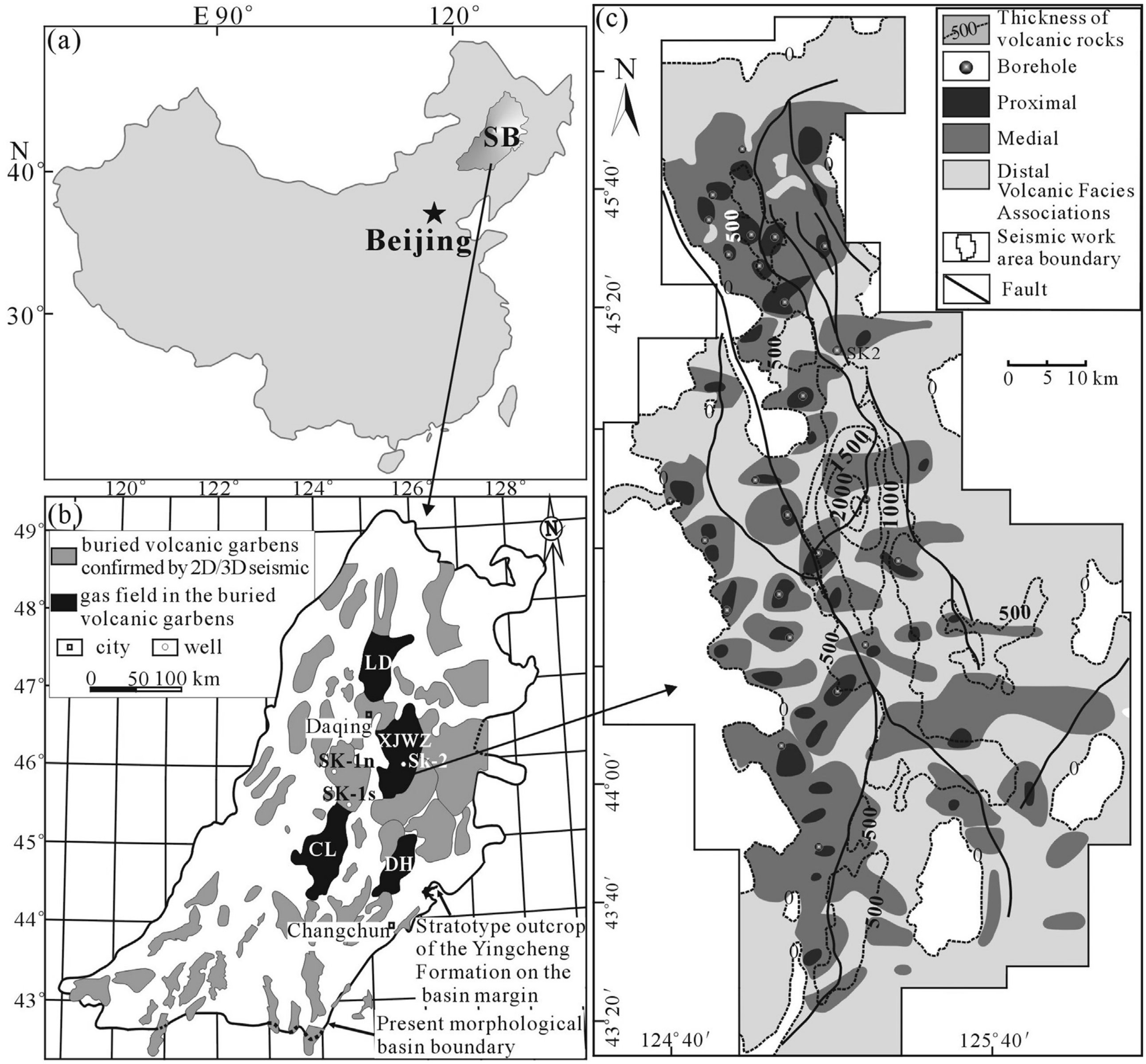

Fig. 1. Volcanic facies associations and stratigraphic isopach of buried paleo-volcanoes of the Yingcheng Formation (Aptian-lower Albian) of northern Songliao Basin (SB). The proximal, medial, and distal facies associations correspond to a paleo-volcano volcanic dome, slope, and edge, respectively. They were recognized both by core and seismic data, as described in detail by Wang and Chen (2015).

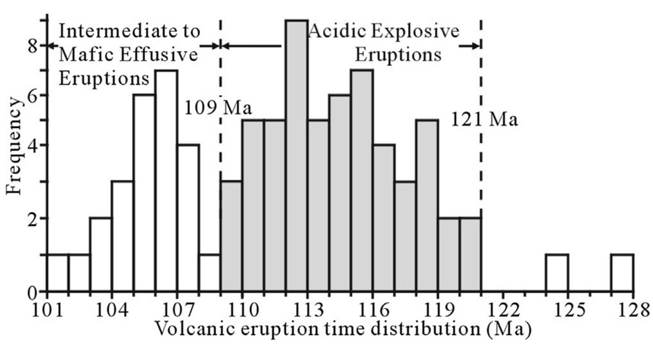

Fig. 2. Eruption time distribution histogram of the Aptian–Albian volcanic rocks in the Songliao Basin (Yingcheng Formation). Volcanic rock zircon ages of 83 sets correspond to those listed in Table 1.

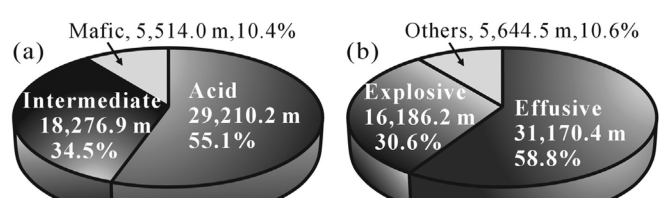

Fig. 3. Lithology (a) and lithofacies associations (b) of the Yingcheng Formation volcanic rocks (Aptian to Albian) in the SB based on 53,001 m of volcanogenic successions from 167 representative boreholes. The explosive and effusive facies are characterized by the textures of volcanic ash fallout and bomb and lava flow structure, respectively. Other facies associations include extrusive, pyroclastic flow and volcanic vent facies, as characterized by Wang et al. (2003).

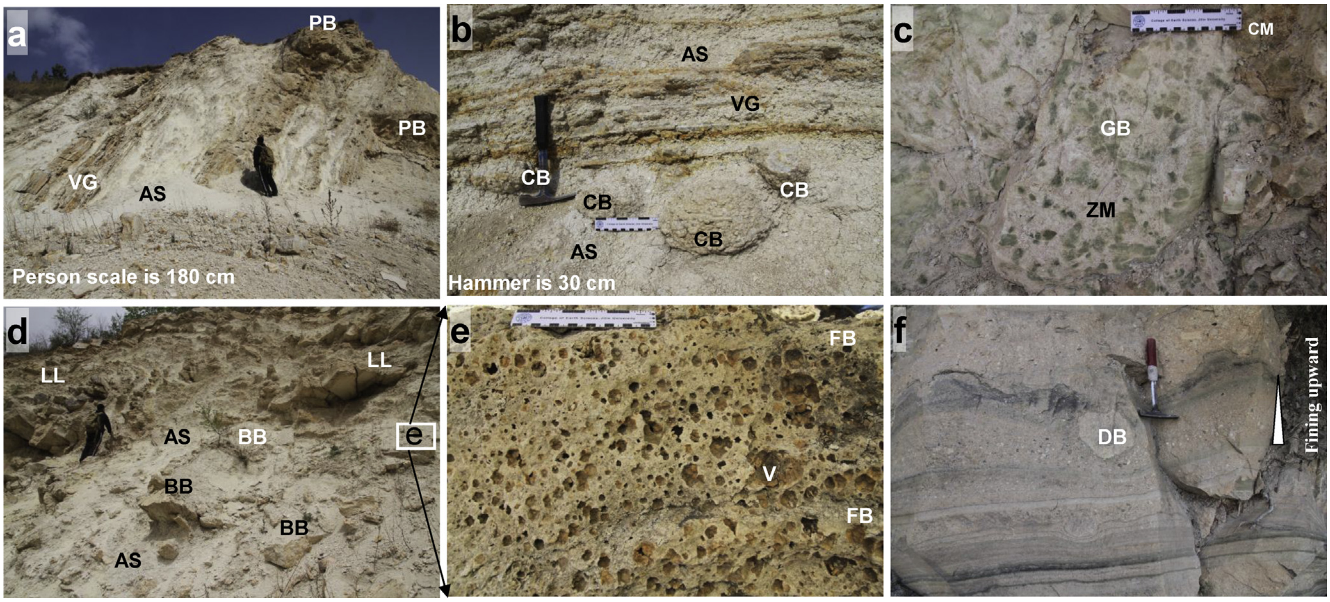

Fig. 4. Phreatomagmatic (a–c) and Plinian (d–f) explosive eruption associations of the Aptian rhyolite in southeastern Songliao Basin (E125°52′, N44°10′). a-White massive volcanic ash (AS) mixed with dark nest-shaped perlite body (PB) and laminated volcanic glass containing volcanic bombs (VG). b-Cauliflower-shaped volcanic bomb (CB) interbedded with laminated volcanic glass (VG) and massive ash (AS). c-Hyaloclastite with green angular volcanic glass breccia (GB) supported by pink zeolite to glassy matrix (ZM). d-White massive volcanic ash (AS) mixed with deformed lava lense (LL) and block and bomb (BB). e-Lavas are vesicle (V)-rich with area porosity of ca. 50% and are interbedded with glassy lava flow bands (FB). f-Pyroclastic surge deposits with graded bedding and drop block structure (DB).

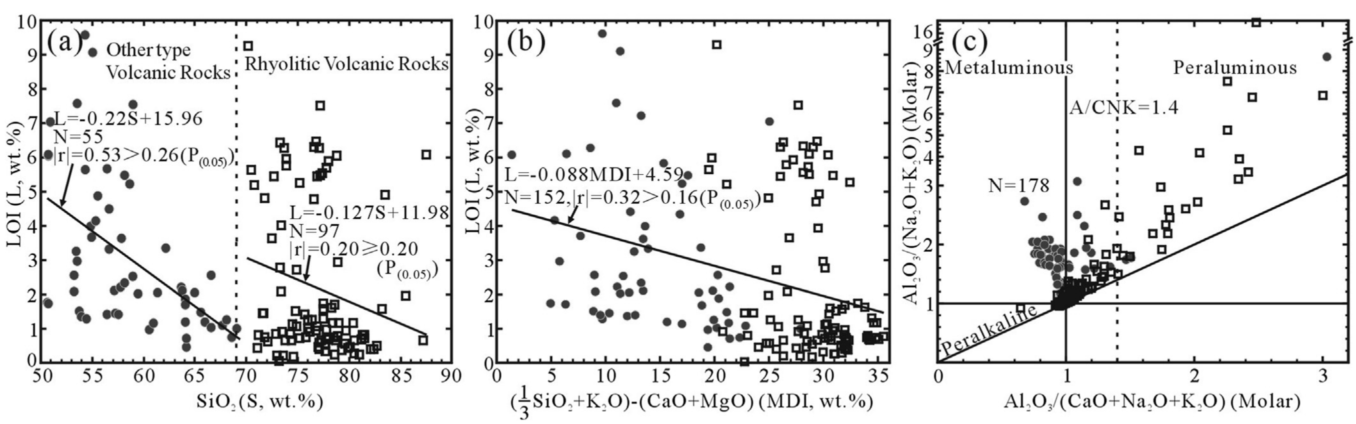

Fig. 5. Lithology (SiO_2 content) (a) and magmatic differentiation index MDI (b) versus total volatile contents contained in the volcanics represented by los-on-ignition (LOI) of the bulk chemical analysis of the rocks. (c)-Shand's index. The acidic rocks are predominantly lower Yingcheng Formation (Y-Fm., 121–109 Ma) and the others are mainly from upper Y-Fm. (108–103 Ma).

eruptions, although minor intermediate to mafic rocks can also be found, most of which were dated between 121 and 109 Ma. The second episode includes predominantly effusive andesitic and mafic volcanic rocks dated between 108 and 103 Ma (Figs. 3 and 4).

The proximal facies associations in Fig. 1 indicate paleo-volcanic explosive centers, as described by Wang and Chen (2015). The densely populated buried volcanic architectures and fault systems shown in Fig. 1 indicate the presence of one large volcano every 80 km^2, which suggests a widespread breaking of the continent and intensive eruptions in the region during the Aptian to Albian. The large scale of strong acidic explosive eruptions began at approximately 199.9–120.2 Ma, and then lasted episodically and decreasingly in magnitude up to ca. 103 Ma. After the early Albian, ca. 108 Ma, they changed into predominantly effusive eruptions with intermediate to mafic lavas (Figs. 3, 5). Plinian and phreatomagmatic eruptions were dominant at the early stage of the eruption, which generated a large volume of fine-grained volcanic ashes, as shown in Fig. 4. The abnormally high abundance of vesicles and gas pipes interbedded with primary lava flow structures suggests that the molten lava experienced degassing processes at a large scale (Fig. 4e). The volcanic rocks of the Y-Fm. contain residual volatile compounds (volatiles) that are hosted in the present-state hard rocks because they generally have a high content of los-on-ignition (LOI) in their bulk chemical composition (Fig. 5). Two separate lithologic groups can be identified within the volcanic rocks of the Y-Fm. Fig. 5a presents rhyolitic volcanic rocks and intermediate to mafic volcanic rocks. Both rock types indicate inverse correlations between silica and LOI weight percentages in which there are declining LOI levels with increasing silicon dioxide concentrations. The magmatic differentiation index (MDI) compared with LOI levels indicates a significant correlation (with a confidence interval of 0.05) between volatile loss and magmatic evolution

Table 1
Zircon U–Pb dating of the Aptian–Albian volcanic rocks of the Yingcheng Formation within and around the Songliao Basin.

No.	Sample no.	Age ± error (Ma)	Sample type and lithology	Sampling location	Dating method & lab	Source
1	P2	111.9 ± 2.2	Outcrops/Rhyolitic tuff	Basin margin	SHRIMP/Beijing SHRIMP Center, Institute of Geology, CAGS, Beijing	this study
2	P5	113.9 ± 0.5	Outcrops/Rhyolite			
3	P6	115.2 ± 0.5	Outcrops/Rhyolitic tuff			
4	P11	114.3 ± 0.5	Outcrops/Rhyolite			
5	YS3	117 ± 1	Drill cores/Rhyolitic tuff	CL graben	LA-ICP-MS/the State Key Laboratory of Geological Processes and Mineral Resources, China University of Geosciences, Wuhan	
6	YS7	118 ± 2	Drill cores/Rhyolitic tuff			
7	XS1	119 ± 3	Drill cores/Trachyte			
8	S101	118 ± 1	Drill cores/Rhyolitic tuff			
9	YS6-2	105	Drill cores/Rhyolite	CL graben	LA-ICP-MS/the State Key Laboratory of Continental Dynamics, Northwest University, Xi'an	Liu, 2014
10	YS7	108 ± 3	Drill cores/Rhyolitic tuff			
11	YS201-1	106 ± 2	Drill cores/Rhyolite			
12	Y1	105 ± 2	Drill cores/Rhyolitic tuff	CL graben	LA-ICP-MS/the State Key Laboratory of Continental Dynamics, Northwest University, Xi'an	Hu, 2013
13	Y3	107 ± 6	Drill cores/Rhyolitic tuff			
14	SN180-1	106 ± 3	Drill cores/Andesite			
15	SN180-2	116 ± 2	Drill cores/Andesite			
16	SN102	112 ± 3	Drill cores/Rhyolitic tuff			
17	Y4	124 ± 1	Drill cores/Granite porphyry			
18	Y6	115 ± 3	Drill cores/Trachyte			
19	L1	105 ± 1	Drill cores/Trachytic tuff			
20	YS4-1	112 ± 1	Drill cores/Trachyte	CL graben	LA-ICP-MS/the State Key Laboratory of Continental Dynamics, Northwest University, Xi'an	Liu et al., 2013
21	YS5-2	104 ± 3	Drill cores/Rhyolite			
22	PRT	127.0 ± 1.0	Outcrops/Rhyolitic tuff	Basin margin	LA-ICP-MS/the Key Laboratory of Continental Dynamics, Northwest University, Xi'an	Shen, 2012
23	LWY-1	115	Outcrops/Rhyolite			
24	HSD	114.7	Outcrops/Andesite		LA-ICP-MS/the State Key Laboratory of Geological Processes and Mineral Resources, China University of Geosciences, Wuhan	
25	XWY	113.7	Outcrops/Andesitic breccia			
26	LWY-2	110.7	Outcrops/Rhyolite			
27	WZ01	114 ± 2	Drill cores/Rhyolite	XJWZ graben	SHRIMP/Curtin University of Technology, Western Australia, and Beijing SHRIMP Center, Institute of Geology, CAGS, Beijing	Zhang et al., 2011
28	WZ03	115 ± 2	Drill cores/Rhyolite			
29	WZ05	112 ± 2	Drill cores/Rhyolite			
30	WZ09	109 ± 2	Drill cores/Andesite			
31	W28	115 ± 2	Drill cores/Rhyolite			
32	WZ30	110 ± 2	Drill cores/Rhyolite			
33	/	104.7 ± 1.8	Drill cores/Rhyolitic ignimbrite	XJWZ graben	LA-ICP-MS/Institute of Geology and Geophysics, Chinese Academy of Sciences, Beijing	Huang et al., 2011
34	/	105.0 ± 3.0	Drill cores/Andesite			
35	/	107.1 ± 4.5	Drill cores/Andesite			
36	/	106.5 ± 0.8	Drill cores/Rhyolite			
37	/	103.5 ± 3.3	Drill cores/Rhyolitic tuff			
38	/	105.3 ± 1.1	Drill cores/Rhyolite			
39	/	103.7 ± 1.1	Drill cores/Rhyolite			
40	/	106.5 ± 2.5	Drill cores/Rhyolite			
41	/	105.4 ± 2.4	Drill cores/Andesite			
42	/	107.7 ± 2.0	Drill cores/Andesite			
43	/	107.9 ± 2.3	Drill cores/Andesite			
44	/	113.8 ± 1.5	Drill cores/Andesite			
45	/	109.4 ± 1.5	Drill cores/Andesite			
46	/	101.4 ± 1.9	Drill cores/Andesite			
47		111.3 ± 1.3	Drill cores/Andesitic tuff			
48		114.0 ± 3.0	Drill cores/Andesitic tuff		SHRIMP/Institute of Geology and Geophysics, Chinese Academy of Sciences, Beijing	
49	/	102.2 ± 2.1	Drill cores/Rhyolitic ignimbrite			
50	/	106.9 ± 2.7	Drill cores/Rhyolite			
51	/	112.1 ± 3.5	Drill cores/Andesite			
52	/	109.2 ± 2.1	Drill cores/Andesite			
53	LS3-1	118.7 ± 4.2	Drill cores/Andesite	LD graben	LA-ICP-MS/Institute of Geology and Geophysics, Chinese Academy of Sciences, Beijing	Jin, Ge, Xue, & Jin, 2011
54	LS3-2	120.2 ± 1.8	Drill cores/Andesite			
55	LS3-3	114 ± 10	Drill cores/Andesite			
56	/	110.6	Outcrops/Rhyolite	Basin margin	SHRIMP/Institute of Geology and Geophysics, Chinese Academy of Sciences, Beijing	Wang, Chen, Liu, Chen, & Lang, 2010
57	D2	104.97 ± 0.74	Drill cores/Rhyolite	CL graben	LA-ICP-MS/the Key Laboratory of Continental Dynamics, Northwest University, Xi'an	Wu, Pu, Han, Cao, & Li, 2010
58	ds7-1	118 ± 2.5	Drill cuttings/Rhyolite	DH graben	LA-ICP-MS/Institute of Geology and Geophysics, Chinese Academy of Sciences, Beijing	Chen, 2009
59	n47-1	113 ± 2	Drill cuttings/Rhyolite			
60	Psc7	116 ± 2	Outcrops/Rhyolite	Basin margin	SHRIMP/Beijing SHRIMP Center, Institute of Geology, CAGS, Beijing	Zhang et al., 2009
61	Psc10	115.2 ± 0.4	Outcrops/Rhyolite			
62	Psc12	117 ± 2	Outcrops/Rhyolite			
63	PLT218	116 ± 3	Outcrops/Rhyolite			
64	PLT195	110 ± 2	Outcrops/Basalt			
65	SN118-1	110 ± 16	Drill cores/Basaltic andesite	CL graben		Pei et al., 2008
66	SN72-5	118 ± 6	Drill cores/Basaltic andesite			

Table 1 (*continued*)

No.	Sample no.	Age ± error (Ma)	Sample type and lithology	Sampling location	Dating method & lab	Source
67	SN56-7	116 ± 1	Drill cores/Trachyandesite		LA-ICP-MS/the Key Laboratory of	
68	L47-1	114 ± 4	Drill cores/Basaltic andesite		Continental Dynamics, Northwest	
69	SN108-2	119 ± 1	Drill cores/Rhyolite		University, Xi'an	
70	XS9a	112.1 ± 1.3	Drill cores/Rhyolite	XJWZ graben	SHIMP/the University of Western	Zhang,
71	XS9b	112.7 ± 1.4	Drill cores/Dacite		Australia, Perth	Chen, et al., 2008
72	XS601-4	111.8 ± 1.9	Drill cores/Rhyolitic ignimbrite	XJWZ graben	SHIMP/the University of Western	Ding et al., 2007
73	XS8-1	111.1 ± 0.9	Drill cores/Felsite		Australia, Perth	
74	XS201-1	111.3 ± 1.5	Drill cores/Rhyolitic tuff			
75	XS502-2	115.1 ± 1.2	Drill cores/Rhyolitic ignimbrite			
76	SP2-1-10	112.8 ± 0.9	Drill cores/Rhyolite			
77	SP2-1-14	113.0 ± 0.8	Drill cores/Dacite			
78	SP202-4	112.0 ± 0.9	Drill cores/Rhyolite			
79	GW04-5-2	117.6 ± 0.5	Outcrops/Dacite	Basin margin	LA-ICP-MS/the Key Laboratory of	Gao, 2007
80	GW04-5-5	106.0 ± 1.6	Outcrops/Rhyolite		Continental Dynamics, Northwest	
81	GW04-555	119.9 ± 0.9	Outcrops/Rhyolite		University, Xi'an	
82	Chao4	106.0 ± 2.8	Drill cores/Rhyolite	XJWZ graben		
83	S202	112 ± 0.9	Drill cores/Rhyolite	XJWZ graben	SHRIMP/Curtin University of Technology, Perth	Zhang et al., 2007

(Fig. 5b). The relationship indicates that volatiles captured in the crystallized rocks and represented by LOI decrease with magmatic differentiation. This characteristic, coupled with the gas-escape structures shown in Fig. 4e, suggests that the volatiles should be predominantly magma-derived. The index of A/CNK (molar ratio of $Al_2O_3/(CaO + Na_2O + K_2O)$ is rock type-dependent, as shown in Fig. 5c, in that most of the intermediate and mafic volcanic rocks are metaluminous with A/CNK values less than 1.08, and most of the rhyolites are peraluminous. Nevertheless, the majority of the volcanic rocks are not significantly altered because only 15% (26/178) of the samples show A/CNK values greater than the critical number of alterations, 1.4 (Siebel et al., 1997), which is equivalent to a value of 58 for the chemical index of alteration (CIA) by Price and Velbel (2003). The 26 samples with A/CNK values ≥ 1.4 were considered to have undergone alteration and have been taken out of the statistics. The other 152 samples used in Fig. 5a, b can be reasonably considered not to have been substantially affected by pedogenic processes. The composition of the volatiles enclosed in the volcanic rocks consists primarily of H_2O, CO_2, CH_4, and other compounds of sulfur, carbon, chlorine, nitrogen, and hydrogen (Table 2). These compounds, when ejected into the atmosphere, could have affected the climate as both greenhouse gases, e.g., CO_2 and CH_4 (Shindell, Schmidt, Miller, & Rind, 2001), and volcanic aerosol from sulfur-rich gases (Metzner et al., 2014).

5. Simultaneous volcanism in northeast Asia

We subdivided the entire continental region into 7 stratigraphic successions involving SB and northeast Asia volcanic rocks. Stratigraphic columns were correlated among different areas, focusing on the Aptian to lower Albian succession (Fig. 6). The marine facies of the Lower Cretaceous sequence decrease rapidly from the continental edge of the Eurasian plate westward to the inland area. The general stratigraphic sequence in the entire region is characterized by volcanogenic successions commonly intercalated by pyroclastics, black shale, and coal beds (Fig. 6), indicating a regional warm climate (Huang, Tan, Yang, Cao, & Li, 1999).

Table 2
Volatile components enclosed in the rhyolite of the Yingcheng Formation, represented by the bulk composition of quartz primary fluid inclusions. Compiled from Feng et al. (2003), Wang, Hou, et al. (2007), Xiao et al. (2011), and Shao, Luo, and Yang (2013).

Vapor phase (mole%)									
	H_2S	CO_2	CO	CH_4	C_2^+	Cl_2	N_2	H_2O	H_2
Max	37.3	99.0	81.4	98.1	36.3	2.9	10.5	99.28	28.4
Mean	7.0	42.1	23.3	55.2	7.1	2.9	2.9	79.5	5.1
Min	0.1	0.16	0.19	0.1	0.1	2.9	0.1	3.98	0.14
Sample number	14	56	17	86	61	1	22	7	9

Table 3 lists the estimation of area, thickness, and volume of the volcanic rocks erupted in the northeast Eurasian continental margin during the Aptian and early Albian. Although the data can only provide a reasonable range for the distribution parameters, the mean values provide reasonable descriptive constraints on the volcanic successions. The area of the continental region is approximately 5.43×10^6 km^2, which is covered by Lower Cretaceous volcanics over an area of approximately 2.34×10^6 km^2. The mean thickness of the volcanics is from 0.35 to 1.2 km, which had been determined by drilling data and outcrop measurements. The actual thickness should be substantially greater than those listed in Table 3 if the related underlying igneous systems are considered. The total volume of the volcanic associations that erupted between the Aptian and early Albian reached a magnitude of at least 1.8×10^6 km^3 on the continental margin. If the LOI value of the SB volcanics in Fig. 5 is used as a reference number for the volatile contents trapped in the volcanic rocks, the total weight of the volatiles hosted in the volcanics of the region would be up to 1.26×10^{14} tons. However, the amount of volatiles ejected into the atmosphere during the Aptian–Albian eruption would be 1.89×10^{14} tons if a value of 1.5 is used as the ratio between the degassing of primary volatiles into air and the host lava inclusion of primary volatiles (Leavitt, 1982). This indicates that the large amount of volcanic gases listed in Table 2 (H_2S, CO_2, CH_4 and analogues) would have been ejected into the atmosphere during the Aptian eruption in the region. Because the eruptions were strong, explosive Plinian and phreatomagmatic eruptions, a large portion of the volcanic gases and ashes would have risen to the stratosphere (Fig. 4) (Bonadonna & Costa, 2013).

6. Discussion

6.1. Isotopic anomalies in marine deposits

It has been demonstrated in geologic history that fallout from tremendous volcanic explosions can change isotopic signatures in marine water and/or sediments. For example, a large drop in seawater $^{87}Sr/^{86}Sr$ during the middle Ordovician was associated with large volcanic ash falls (Young, Saltzman, Foland, Linder, &

Table 3
Estimation of area, thickness, volume, and total volatiles ejected from the Aptian to Albian volcanism of the Songliao Basin and northeast Asia (SB-V).

Stratigraphic division	Total area ($\times 10^6$ km^2)	Volcanic area[a] ($\times 10^6$ km^2)	Volcanic thickness[b] (km)	Volcanic volume[c] ($\times 10^6$ km^3)	Volatiles hosted in volcanics[d]	Volatiles released into atmosphere[e]
					($\times 10^{11}$ ton) Min/Mean/Max	
①Sikhote-Alin	0.46	0.253	1.2	0.304	79/198/474	119/297/711
②Sanjiang B.-Yanji B.	0.75	0.338	0.8	0.271	71/176/423	107/264/635
③Songliao B.-Jiayin B.	0.46	0.299	0.9	0.269	70/175/420	105/263/630
④Great Xing'an Mountain Belt	0.42	0.231	1.2	0.277	72/180/432	108/270/648
⑤Hai-Ta B.-Erlian B.	0.38	0.228	1.2	0.274	71/178/427	107/267/641
⑥Circum-Mongolia arc Belt	1.34	0.670	0.5	0.335	87/218/523	131/327/785
⑦Mongolia-Okhotsk Belt	1.62	0.324	0.35	0.113	29/132/176	44/198/164
Total	5.43	2.343		1.843	479/1257/2875	721/1886/4214

[a] Volcanic area was estimated based on Karsakov and Zhao (2001), Ren et al. (2013), and Petrov et al., (2014).
[b] Volcanic thickness is based on the stratigraphic columns in Fig. 6①–⑦.
[c] Volatiles hosted in the volcanic rocks = volcanic volume × volatile %w of rock × rock density.
[d] We chose volcanic volatile percentage of Min = 1%, Mean = 2.5%, Max = 6%, and Rock Density = 2.6 g/cm^3 for calculations using data in Fig. 5a.
[e] Volatiles released into atmosphere = Volatiles hosted in the volcanics × 1.5 according to the ratio between rock-enclosed volatiles and volatiles released into air (Leavitt, 1982).

Kump, 2009). The initial ratio of $(^{87}Sr/^{86}Sr)_i$ of the Aptian volcanic rocks and fallout exploded from the Songliao Basin and adjacent area (in short SB-V) ranges from 0.70187 to 0.70660, and the ratios of $(^{206}Pb/^{204}Pb)_i$, $(^{207}Pb/^{204}Pb)_i$, and $(^{208}Pb/^{204}Pb)_i$ from the SB-V range between 17.70 and 18.41, 15.51 and 15.58, and 37.53 and 38.22, respectively. The shift in $(^{87}Sr/^{86}Sr)_i$ is commonly from the pre-excursion value of 0.70750 to the most negative value of 0.70720 recorded in marine deposits during 125–113 Ma (Jenkyns, 2010). All of the shifting values are within the pre-Aptian high level of 0.70750 and the mean value 0.70433 for the SB-V. Similarly, the lead isotopic record of Barremian–Aptian marine deposits indicates values between the pre-excursion high values of 18.8 $(^{206}Pb/^{204}Pb)_i$, 15.66 $(^{207}Pb/^{204}Pb)_i$, and 38.7 $(^{208}Pb/^{204}Pb)_i$ and the mean values of 18.15, 15.55, and 37.98, respectively, for the SB-V (Fig. 7). It is therefore reasonable to conclude that rhyolitic volcanic ash falls from the violent Aptian eruptions of the SB-V must have contributed to the isotopic signatures of the contemporaneous marine deposits according to the following three factors. The first factor is that the time period matched with each of the two events, the SB-V and negative isotope excursions of marine deposits in the Mid-Pacific. The second factor is space affinity because the SB-V volcanoes were developed on the active continental margin of the circum-Pacific domain. The third factor is that the Aptian eruptions of the SB-V were mainly strong and explosive, and therefore generated a high volume of fine-grained volcanic ash that could potentially reach a high altitude in the atmosphere. It should be noted that the SB-V appears to have had an insignificant impact on the strontium isotope excursion after 112 Ma (Fig. 7), which may be appropriately explained by the changes in eruption types. The Aptian eruptions were acidic and predominantly explosive, with a large portion consisting of fine-grained volcanic ash (Fig. 4). However, following a short eruption quiescent episode, the Albian eruptions were primarily intermediate and mafic effusive eruptions, with much less volcanic ash. In addition to the eruption types, the transport of volcanic ash would be through wind-driven processes (Man, Zhou, & Jungclaus, 2014), and the dust fall from the volcanic eruptions would be randomly deposited. As a result, the volcanic ash contribution to marine deposits should be expected to be irregular. This characteristic of volcanic fallout may better explain the contrast in isotopic signatures of lead and osmium recorded in the Aptian marine deposits from both the Pacific and Italy (Bottini et al., 2012; Kuroda et al., 2011) because in some cases, the signatures may be influenced by volcanic ash components and be controlled by paleo-wind direction rather than by paleo-ocean circulation. Further work would be required to consider the tephra chronology and geochemical correlation between volcanic ash of the SB-V and possible ash components enclosed in the simultaneous marine deposits.

6.2. Global climate change and OAE-1a

The link between volcanism and climate is complicated (Zielinski, 2000). Volcanic eruptions may cause climate change in different ways (Zielinski et al., 1994), either through cooling resulting from scattered solar radiation caused by both volcanic aerosol and ash dust, especially for the Plinian eruptions (Metzner et al., 2014), or through warming resulting from the greenhouse gases ejected into the atmosphere (Self, Widdowson, Thordarson, & Jay, 2006). However, the cooling impact on climate would typically be shorter and stronger relative to the long-term accumulative greenhouse effect (Moriya, 2011; Robock, 2000; Shindell, Schmidt, Mann, & Faluvegi, 2004; Stenchikov et al., 2006). The Aptian volcanic eruptions in the Songliao Basin and northeast Asia (SB-V) were volatile-rich Plinian and phreatomagmatic eruptions that ejected a large volume of volcanic ash and gases into the atmosphere (Figs. 2, 4), including both aerosol and greenhouse gases (Table 2). Transient global cooling at the onset of the early Aptian OAE-1a was indicated by isotopes of contemporaneous shallow marine carbonates and was probably triggered by changes in radiative forcing (Kuhnt, Holbourn, & Moullade, 2011). DeBond, Oakes, Paytan, and Wortmann (2012) proposed a model regarding the forcing of volcanic particles in the global sulphur cycle based on the isotopic signatures of marine deposits at Ocean Drilling Program (ODP) site 765 in the western Indian Ocean. This model assumed a sevenfold increase in the mantle degassing rate from 121 Ma to 120 Ma. The extremely strong, explosive eruptions of the SB-V began at approximately 119.9–120.2 Ma (Table 1), which is in agreement with the timing of the transient global cooling and the worldwide abrupt isotopic changes in marine deposits. A magnitude of ca. 1.89×10^{14} tons of volcanic volatiles was ejected into the atmosphere from the SB-V Aptian eruption (Table 3) and a large portion of them were gases that form aerosols, such as hydrogen sulfide (Table 2). In addition to volatiles, a large amount of volcanic dust was generated and a large portion of the dust would have potentially entered the stratosphere (Fig. 4). We therefore infer that the SB-V must have played a role in the early Aptian global climate changes by causing changes in solar radiation and global circulation patterns of climate, and modifications of the global carbon cycle, which may be similar to the observed modern processes described by Langmann (2014).

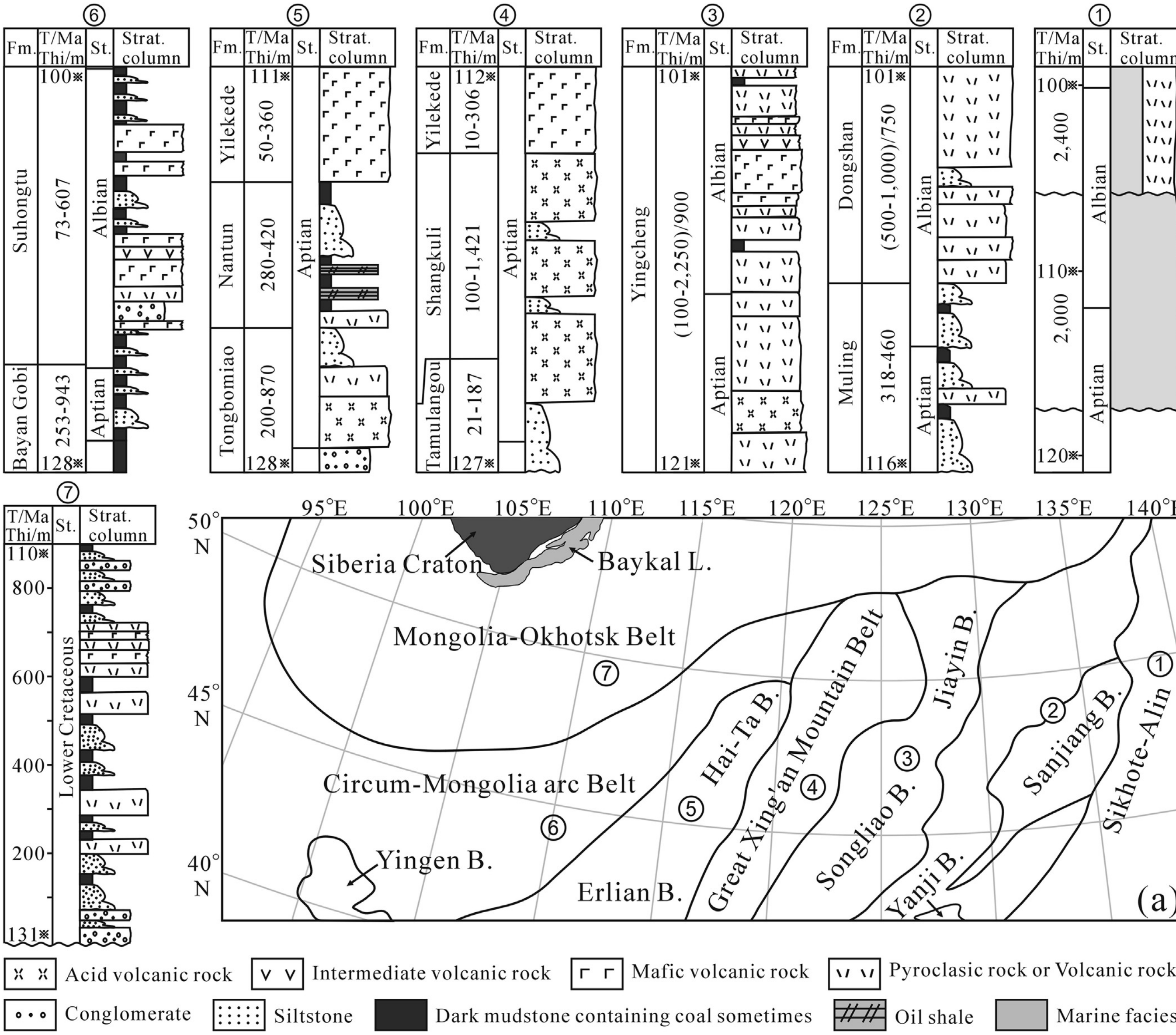

Fig. 6. Aptian–Albian volcanism in the Songliao Basin and northeast Asia (SB-V). ① to ⑦-Stratigraphic correlation in northeast Asia focusing on the equivalent Yingcheng Formation (ca. 121 Ma–103 Ma). (a)-Stratigraphic subdivision and distribution of the SB-V. The stratigraphic columns are compiled according to ①;-Karsakov & Zhao, 2001; Kirillova, 2003; ②;-Sha, Hirano, Yao, & Pan, 2008; HGS, 1993; ③;-Wang, Liu, et al., 2002a; Wang, Ren, et al., 2002b; ④;-Fan, Guo, Wang, & Lin, 2003; Zhang, Ge, et al., 2008; ⑤;-Liu, Huang, & Ye, 2004; A et al., 2013; ⑥;-Meng, 2003; Guo, Yu, & Fan, 2002; ⑦;-Graham et al., 2001.

6.3. Comparison between the OJP and the SB-V

The area of the Aptian–Albian volcanic province in the Songliao Basin and northeast Asia (SB-V) is comparable in size to the OJP but formed in two phases within 20 Myr (Fig. 2), whereas the emplacement of the OJP seems to have occurred only in the early Aptian (Fitton et al., 2004). Thus, it appears that the northeast Asia volcanism might have been important for the long-term climatic trends but not as important in the short term, such as during the OAE-1a. However, the SB-V strong, explosive Plinian and phreatomagmatic eruptions (Fig. 4) could raise the massive clouds of ejected dust and gases high enough to reach the stratosphere (Bonadonna & Costa, 2013), which would have the capability of cooling global climate for several years after each eruption similar to the recent cases described by Zielinski (2000). We therefore infer that the transient global cooling at the onset of the OAE-1a (~120 Ma, Kuhnt et al., 2011) could be impacted to some extent by the SB-V because the acidic explosive mega-eruptions in the SB also began at approximately 119.9–120.2 Ma (see Table 1 and Fig. 2).

7. Conclusions

7.1. The SB-V

The time span, lithology, eruption type, and magnitude of the SB-V are as follows. The Aptian–Albian volcanism was widespread in the Songliao Basin and northeast Asia, covering an area of ca. 2.3×10^6 km^2, which may match the magnitude of the contemporaneous Ontong Java Plateau (OJP) flood basalt in the western Pacific (area of 2.0×10^6 km^2, Wignall, 2001; Fitton et al., 2004). The mean thickness of the SB-V confirmed by borehole and outcrop

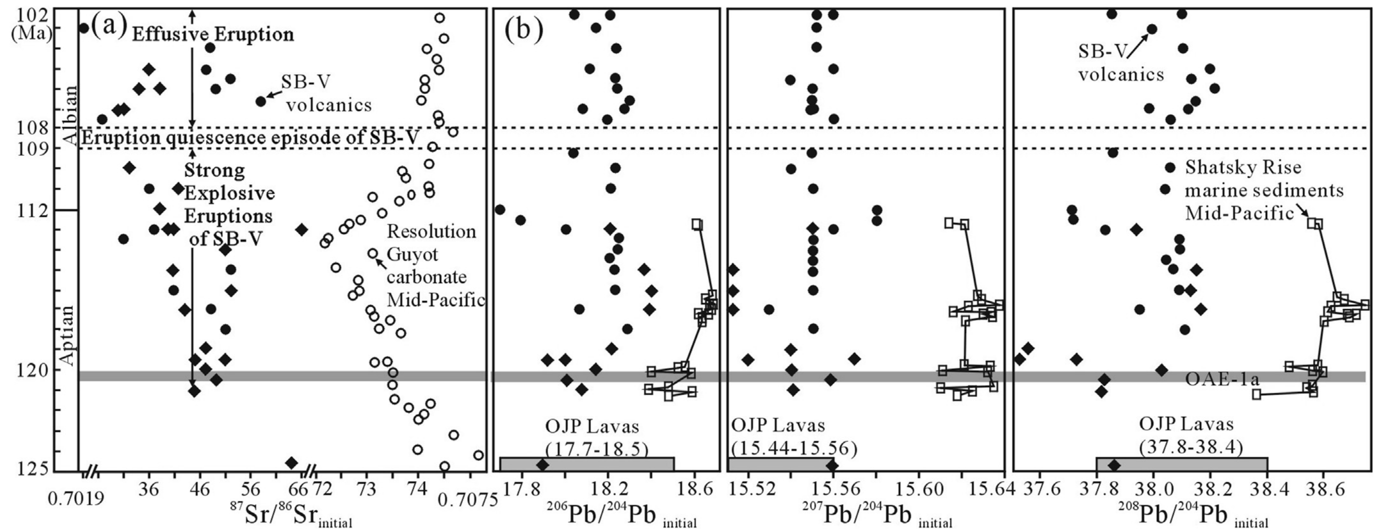

Fig. 7. Correlation of strontium and lead isotopes between volcanic rocks/ashes in the Songliao Basin and simultaneous marine deposits from the Mid-Pacific. (a)-Comparison with the Cretaceous platform carbonates of Resolution Guyot (Jenkyns & Wilson, 1999). (b)-Comparison with the core samples from ODP site 1207 (Kuroda et al., 2011). The location of OAE-1a is determined by the C-zone stratigraphy in Menegatti et al. (1998) and corresponding absolute ages are based on DeBond et al. (2012), which are marked by the grey bar. Strontium and lead isotope data of volcanic rocks/ashes in the SB are from Wang et al. (2006) and Meng, Liu, and Cui (2013) (the 10 diamonds), and this study (the 24 dots).

data ranges from 0.35 to 1.2 km and has a total volume of at least 1.8×10^6 km^3. If the underlying igneous systems are considered, the total volume of the SB-V would be much greater. The intense, explosive volcanic eruptions occurred successively from 121 Ma to 109 Ma. The large scale of the strong, explosive eruptions of the SB-V resulted in a large volume of volcanic ash and at least 1.89×10^{14} tons of volcanic volatiles were ejected into the atmosphere (Table 3).

7.2. Volcanic ash of the SB-V and isotopic anomalies of contemporaneous marine deposits

The strontium isotopic excursion of the Aptian–Albian (121–113 Ma) in marine carbonates from the Mid-Pacific shift from radiogenic values of $(^{87}Sr/^{86}Sr)_i = 0.70443$ towards the mean magmatic value of the SB-V, $(^{87}Sr/^{86}Sr)_i = 0.70720$. Similarly, lead isotopes in Pacific marine deposits showed shifting values between pre-excursion levels and mean magmatic values of the SB-V (Fig. 7). It was therefore probable that volcanic dust contributed to the isotopic record of marine deposits, considering the time, space, and eruption type of the SB-V.

7.3. SB-V effect on the Aptian global climate change and OAE-1a

The massive volcanic dust and degassing compounds ejected high into the atmosphere from the SB-V began in the early Aptian (119.9–120.2 Ma), which was the same time of the transient global cooling at the onset of the OAE-1a (Kuhnt et al., 2011). The abrupt cooling could be attributed to an increase in the reflection of sunlight caused by a dramatic increase of the atmospheric burden of aerosol/volcanic dust, partly due to the contemporaneous SB-V. The greenhouse gases outgassed from the SB-V 121–109 Ma (Figs. 2, 4) may have played a role in the subsequent long-term global warming and increasing partial pressure of CO_2 (pCO_2) in the atmosphere from the Aptian to the early Albian.

Acknowledgments

The project was sponsored by the National Natural Science Foundation of China (Grant No. 41472304), and the National Basic Research Program of China (973 Program, Grant No. 2012CB822002). Thanks to Dr. E. Koutsoukos and two anonymous reviewers for their constructive comments on the manuscript.

References

A, M. N., Zhang, F. Q., Yang, S. F., Chen, H. L., Batt, G. E., Sun, M. D., et al. (2013). Early Cretaceous provenance change in the southern Hailar Basin, northeastern China and its implication for basin evolution. *Cretaceous Research, 40*, 21–42. http://dx.doi.org/10.1016/j.cretres.2012.05.005.

Bonadonna, C., & Costa, A. (2013). Plume height, volume, and classification of explosive volcanic eruptions based on the Weibull function. *Bulletin of Volcanology, 75*(742). http://dx.doi.org/10.1007/s00445-013-0742-1.

Bottini, C., Cohen, A. S., Erba, E., Jenkyns, H. C., & Coe, A. L. (2012). Osmium-isotope evidence for volcanism, weathering, and ocean mixing during the early Aptian OAE 1a. *Geology, 40*, 583–586. http://dx.doi.org/10.1130/G33140.1.

van Breugel, Y., Schouten, S., Tsikos, H., Erba, E., Price, G. D., & Sinninghe Damsté, J. S. (2007). Synchronous negative carbon isotope shifts in marine and terrestrial biomarkers at the onset of the early Aptian oceanic anoxic event 1a: evidence for the release of ^{13}C-depleted carbon into the atmosphere. *Paleoceanography, 22*, PA1210. http://dx.doi.org/10.1029/2006PA001341.

Chen, J. S. (2009). *The genesisi of volcanic rocks of Ying Cheng group in southern Songliao Basin* (Master thesis). Changchun: Jilin University (in Chinese with English abstract).

Chen, F., Hegner, E., & Todt, W. (2000). Zircon ages and Nd isotopic and chemical compositions of orthogneisses from the Black Forest, Germany: evidence for a Cambrian magmatic arc. *International Journal of Earth Sciences, 88*, 791–802. http://dx.doi.org/10.1007/s005310050306.

Daqing Petroleum Geology Committee (DPGC). (1993). *Petroleum geology of China* (Vol. 2, p. 875). Beijing: Petroleum Industry Press (in Chinese).

DeBond, N., Oakes, R. L., Paytan, A., & Wortmann, U. G. (2012). Early Aptian carbon and sulphur isotope signatures at ODP Site 765. *Isotopes in Environmental and Health Studies, 48*, 180–194. http://dx.doi.org/10.1080/10256016.2012.659732.

Ding, R. X., Shu, P., Ji, X. Y., Qu, Y. M., Cheng, R. H., & Zhang, B. (2007). SHRIMP ziron U-Pb age and geological meaning of reservoir volcanic rocks in Qingshen Gas Field of the Songliao Basin, NE China. *Journal of Jilin University (Earth Science Edition), 37*, 525–530 (in Chinese with English abstract).

Fan, W. M., Guo, F., Wang, Y. J., & Lin, G. (2003). Late Mesozoic calc-alkaline volcanism of post-orogenic extension in the northern Da Hinggan Mountains, northeastern China. *Journal of Volcanology and Geothermal Research, 121*, 115–135. http://dx.doi.org/10.1016/S0377-0273(02)00415-8.

Feng, Z. Q., Liu, J. Q., Wang, P. J., Chen, S. M., Feng, Z. H., & Tong, Y. (2011). New oil and gas exploration field: volcanic hydrocarbon reservoirs-enlightenment from the discovery of the large gas field in Songliao Basin. *Chinese Journal of Geophysics, 54*, 269–279 (in Chinese with English abstract).

Feng, Z. H., Ren, Y. G., Wang, C., Li, J. K., Wang, X., & Guan, Q. H. (2003). Study on inclusion of deep buried igneous reservoir and forming period of gas pool in Songliao Basin. *Natural Gas Geoscience, 14*, 436–442 (in Chinese with English abstract).

Fitton, J. G., Mahoney, J. J., Wallace, P. J., & Saunders, A. D. (2004). *Origin and* *evolution of the Ontong Java Plateau: Introduction* (pp. 1–8). London: Geological Society. Special Publications 229 http://dx.doi.org/10.1144/GSL.SP.2004.229.01.01.

Föllmi, K. (2012). Early Cretaceous life, climate and anoxia. *Cretaceous Research, 35*, 230–257. http://dx.doi.org/10.1016/j.cretres.2011.12.005.

Gao, Y. (2007). *Chronology and geochemistry of Mesozoic volcanic rocks in southeastern Songliao Basin* (Master thesis). Changchun: Jilin University (in Chinese with English abstract).

Graham, S. A., Hendrix, M. S., Johnson, C. L., Badamgarav, D., Badarch, G., Amory, J., et al. (2001). Sedimentary record and tectonic implications of Mesozoic rifting in southeast Mongolia. *Geological Society of America Bulletin, 113*, 1560–1579. http://dx.doi.org/10.1130/0016-7606(2001)113<1560:SRATIO>2.0.CO;2.

Guo, Y. R., Yu, J. M., & Fan, T. L. (2002). Evolution and sequence stratigraphic framework of Lower Cretaceous in Chagan depression. *Oil and Gas Geology, 23*, 166–169 (in Chinese with English abstract).

Heilongjiang Geological Survey (HGS). (1993). *Regional geology of Heilongjiang province of China* (p. 734). Beijing: Geology Press (in Chinese).

Hu, C. X. (2013). Structural characteristics and post-Cretaceous tectonic evolution of the Changling rift. *Oil & Gas Geology, 34*, 229–235 (in Chinese with English abstract).

Huang, Q. H., Tan, W., Yang, H. C., Cao, H. H., & Li, Q. (1999). Stratigraphic succession and chronostrata of Cretaceous in Songliao Basin. *Petroleum Geology & Oilfield Development in Daqing, 18*, 9–11 (in Chinese with English abstract).

Huang, Q. H., Zheng, Y. L., Yang, M. J., Li, X. J., Han, M. X., & Chen, C. R. (2011). On Cretaceous paleoclimate in the Songliao Basin. *Acta Micropalaeontologica Sinica, 16*, 95–103 (in Chinese with English abstract).

Inner-Mongolia Geological Survey (IGS). (1991). *Regional geology of Inner-Mongolia autonomous region of China* (p. 725). Beijing: Geology Press (in Chinese).

Jenkyns, H. C. (2010). Geochemistry of oceanic anoxic events. *Geochemistry Geophysics Geosystems, 11*. http://dx.doi.org/10.1029/2009GC002788.

Jenkyns, H. C., & Wilson, P. A. (1999). Stratigraphy, paleoceanography, and evolution of Cretaceous Pacific guyots: relics from a greenhouse Earth. *American Journal of Science, 299*, 341–392. http://dx.doi.org/10.1.1.507.1760.

Jin, X., Ge, W. C., Xue, Y. F., & Jin, Y. D. (2011). Zircon U-Pb ages and Hf isotopic composition of volcanic rocks from Well Linshen 3 in Songliao Basin. *Global Geology, 30*, 7–17 (in Chinese with English abstract).

Karsakov, L. P., Zhao, C. J.., 2001. Tectonic Map of the Central Asia-Pacific Belts Junction Area. Khobarovsk: Yu. A. Kosygin Institute of Tectonics and Geophisics, Far Eastern Branch, Russian Academy of Science.

Keller, G. (2008). Cretaceous climate, volcanism, impacts, and biotic effects. *Cretaceous Research, 29*, 754–771. http://dx.doi.org/10.1016/j.cretres.2008.05.030.

Keller, C. E., Hochuli, P. A., Weissert, H., Bernasconi, S. M., Giorgioni, M., & Garcia, T. I. (2011). A volcanically induced climate warming and floral change preceded the onset of OAE1a (Early Cretaceous). *Palaeogeography, Palaeoclimatology, Palaeoecology, 305*, 43–49. http://dx.doi.org/10.1016/j.palaeo.2011.02.011.

Khanchuk, A. I. (2012). *Sedimentary basins of East Russia* (p. 360). Vladivolstok: Dalnauka Press (in Russia with English figures).

Kirillova, G. L. (2003). Late Mesozoic-Cenozoic sedimentary basins of active continental margin of southeast Russia: paleogeography, tectonics, and coal-oil-gas presence. *Marine and Petroleum Geology, 20*, 385–397. http://dx.doi.org/10.1016/S0264-8172(03)00046-1.

Kuhnt, W., Holbourn, A., & Moullade, M. (2011). Transient global cooling at the onset of early Aptian oceanic anoxic event (OAE) 1a. *Geology, 39*, 323–326. http://dx.doi.org/10.1130/G31554.1.

Kuroda, J., Tanimizu, M., Hori, R. S., Suzuki, K., Ogawa, N. O., Tejada, M. L. G., et al. (2011). Lead isotopic record of Barremian-Aptian marine sediments: implications for large igneous provinces and the Aptian climatic crisis. *Earth and Planetary Science Letters, 307*, 126–134. http://dx.doi.org/10.1016/j.epsl.2011.04.021.

Langmann, B. (2014). On the role of climate forcing by volcanic sulphate and volcanic ash. *Advances in Meteorology, 2014*. http://dx.doi.org/10.1155/2014/340123.

Larson, R. L., & Erba, E. (1999). Onset of the mid-Cretaceous greenhouse in the Barremian-Aptian: igneous events and the biological, sedimentary, and geochemical responses. *Paleoceanography, 14*, 663–678. http://dx.doi.org/10.1029/1999PA900040.

Leavitt, S. W. (1982). Annual volcanic carbon dioxide emission: an estimate from eruption chronologies. *Environmental Geology, 4*, 15–21. http://dx.doi.org/10.1007/BF02380495.

LeMaitre, R. W. (1989). *A classification of igneous rocks and a glossary of terms* (p. 193). Oxford: Blackwell.

Liu, W. (2014). *Age, geochemistry and petrogenesis of the Yingcheng Formation from Changling depression in the Songliao Basin* (Master thesis). Changchun: Jilin University (in Chinese with English abstract).

Liu, Z. W., Huang, Q. H., & Ye, D. Q. (2004). The Cretaceous ostrcoda assemblages and its biostratigraphic characteristics in the Hailaer Basin. *Acta Micropalaeontologica Sinica, 21*, 309–321 (in Chinese with English abstract).

Liu, W., Sun, D. Y., Li, R. L., Liu, M. L., Wen, S. F., Zhang, X., et al. (2013). Chronology and petrogenesis of volcanic rocks in Yingcheng Formation from Changling depression in Songliao Basin. *Global Geology, 32*, 522–530 (in Chinese with English abstract).

Man, W., Zhou, T., & Jungclaus, J. H. (2014). Effects of large volcanic eruptions on global summer climate and East Asian monsoon changes during the last millennium: analysis of MPI-ESM simulations. *Journal of Climate, 27*, 7394–7409. http://dx.doi.org/10.1175/JCLI-D-13-00739.1.

Menegatti, A. P., Weissert, H., Brown, R. S., Tyson, R. V., Farrimond, P., Strasser, A., et al. (1998). High-resolution $\delta^{13}C$ stratigraphy through the Early Aptian "Livello selli" of the Alpine Tethys. *Paleoceanography, 13*, 530–545. http://dx.doi.org/10.1029/98PA01793.

Meng, Q. R. (2003). What drove late Mesozoic extension of the northern China-Mongolia tract? *Tectonophysics, 369*, 155–174. http://dx.doi.org/10.1016/S0040-1951(03)00195-1.

Meng, F. C., Liu, J. Q., & Cui, Y. (2013). Petrogenesis and crypto-explosive mechanism of trachte in Yingcheng Formation of Xujiawei fault depression, Songliao Basin, NE China. *Journal of Jilin University (Earth Science Edition), 43*, 704–715 (in Chinese with English abstract).

Metzner, D., Kutterolf, S., Toohey, M., Timmreck, C., Niemeier, U., Freundt, A., et al. (2014). Radiative forcing and climate impact resulting from SO_2 injections based on a 200,000-year record of Plinian eruptions along the Central American Volcanic Arc. *International Journal of Earth Sciences, 103*, 2063–2079. http://dx.doi.org/10.1007/s00531-012-0814-z.

Misumi, K., Yamanaka, Y., & Tajika, E. (2009). Numerical simulation of atmospheric and oceanic biogeochemical cycles to an episodic CO_2 release event: implications for the cause of mid-Cretaceous Ocean Anoxic Event-1a. *Earth and Planetary Science Letters, 286*, 316–323. http://dx.doi.org/10.1016/j.epsl.2009.06.045.

Moriya, K. (2011). Development of the Cretaceous greenhouse climate and the oceanic thermal structure. *Paleontological Research, 15*, 77–88. http://dx.doi.org/10.2517/1342-8144-15.2.077.

Pei, F. P., Xu, W. L., Yang, D. B., Ji, W. Q., Yu, Y., & Zhang, X. Z. (2008). Mesozic volcanic rocks in the southern Songliao Basin: zircon U-Pb ages and their constraints on the nature of basin basement. *Earth Science, 33*, 603–617 (in Chinese with English abstract).

Petrov, O. V., Leonov, Y. G., & Pospelov, I. I. (2014). *Tectonic map of northern-central-eastern asia and adjacent areas at 1:2,500,000 scale*. Saint Petersburg: VSEGEI Printing House.

Price, J. R., & Velbel, M. A. (2003). Chemical weathering indices applied to weathering profiles developed on heterogeneous felsic metamorphic parent rocks. *Chemical Geology, 202*, 397–416. http://dx.doi.org/10.1016/j.chemgeo.2002.11.001.

Ren, J. S., Niu, B. G., Wang, J., Jin, X. C., & Xie, L. Z. (2013). *International geological map of asia (IGMA5000), 1: 5 million*. Beijing: Geological Press.

Ren, J. Y., Tamaki, K., Lia, S., & Zhang, J. X. (2002). Late Mesozoic and Cenozoic rifting and its dynamic setting in Eastern China and adjacent areas. *Tectonophysics, 344*, 175–205. http://dx.doi.org/10.1016/S0040-1951(01)00271-2.

Robock, A. (2000). Volcanic eruptions and climate. *Reviews of Geophysics, 38*, 191–219. http://dx.doi.org/10.1029/1998RG000054.

Self, S., Widdowson, M., Thordarson, T., & Jay, A. E. (2006). Volatile fluxes during flood basalt eruptions and potential effects on the global environment: a Deccan perspective. *Earth and Planetary Science Letters, 248*, 518–532. http://dx.doi.org/10.1016/j.epsl.2006.05.041.

Sha, J. G., Hirano, H., Yao, X. G., & Pan, Y. H. (2008). Late Mesozoic transgressions of eastern Heilongjiang and their significance in tectonics, and coal and oil accumulation in northeast China. *Palaeogeography, Palaeoclimatology, Palaeoecology, 263*, 119–130. http://dx.doi.org/10.1016/j.palaeo.2008.02.008.

Shao, H. M., Luo, J. L., & Yang, Y. F. (2013). Origin and quality evolution of volcanic reservoir in the Yingcheng Formation, Songliao Basin. *Chinese Journal of Geology, 48*, 1187–1203 (in Chinese with English abstract).

Shen, Y. J. (2012). *Pyroclastic rock of Yingcheng Formation in Songliao Basin: Facies. Architecture. Application* (Ph.D thesis). Changchun: Jilin University (in Chinese with English abstract).

Shindell, D. T., Schmidt, G. A., Mann, M. E., & Faluvegi, G. (2004). Dynamic winter climate response to large tropical volcanic eruptions since 1600. *Journal of Geophysical Research, 109*. D05104 http://dx.doi.org/10.1029/2003JD004151.

Shindell, D. T., Schmidt, G. A., Miller, R. L., & Rind, D. (2001). Northern Hemisphere winter climate response to greenhouse gas, ozone, solar, and volcanic forcing. *Journal of Geophysical Research, 106*, 7193–7210. http://dx.doi.org/10.1029/2000JD900547.

Siebel, W., Raschka, H., Irber, W., Kreuzer, H., Lenz, K.-L., Höhndorf, A., et al. (1997). Early Palaeozoic acid magmatism in the Saxothuringian Belt: new insights from a geochemical and isotopic study of orthogneisses and metavolcanic rocks from the Fichtelgebirge, SE Germany. *Journal of Petrology, 38*, 203–230. http://dx.doi.org/10.1093/petroj/38.2.203.

Sigl, M., McConnell, J. R., Layman, L., Maselli, O., McGwire, K., Pasteris, D., et al. (2013). A new bipolar ice core record of volcanism from WAIS Divide and NEEM and implications for climate forcing of the last 2000 years. *Journal of Geophysical Research, 118*, 1151–1169. http://dx.doi.org/10.1029/2012JD018603.

Stenchikov, G., Hamilton, K., Stouffer, R. J., Robock, A., Ramaswamy, V., Santer, B., et al. (2006). Arctic oscillation response to volcanic eruptions in the IPCC AR4 climate models. *Journal of Geophysical Research, 111*. D07107 http://dx.doi.org/10.1029/2005JD006286.

Wang, P. J., & Chen, S. M. (2015). Cretaceous volcanic reservoirs and their exploration in the Songliao Basin, NE China. *AAPG Bulletin, 99*, 499–523. http://dx.doi.org/10.1306/09041413095.

Wang, P. J., Chen, F. K., Chen, S. M., Siebel, W., & Satir, M. (2006). Geochemical and Nd-Sr-Pb isotopic composition of Mesozoic volcanic rocks in the Songliao basin, NE China. *Geochemical Journal, 40*, 149–159. http://dx.doi.org/10.2343/geochemj.40.149.

Wang, P. J., Chen, S. M., Liu, W. Z., Chen, H. L., & Lang, Y. Q. (2010). Chronology, petrology and geochemistry of the Cretaceous cryto-explosive breccia-bearing volcanic rocks: implications for volcanic resvoir and tectonics of the Songliao

Basin, NE China. *Acta Petrologica Sinica, 26*, 33–46 (in Chinese with English abstract).

Wang, P. J., Chi, Y. L., Liu, W. Z., Cheng, R. H., Shan, X. L., & Ren, Y. G. (2003). Volcanic facies of the Songliao Basin: classification, characteristics and reservoir significance. *Journal of Jilin University (Earth Science Edition), 33*, 449–456 (in Chinese with English abstract).

Wang, P. J., Hou, Q. J., Wang, K. Y., Chen, S. M., Cheng, R. H., Liu, W. Z., et al. (2007). Discovery and significance of high CH_4 primary fluid inclusions in reservoir volcanic rocks of the Songliao Basin, NE China. *Acta Geologica Sinica, 81*, 113–120.

Wang, Y. D., Huang, C. M., Sun, B. N., Quan, C., Wu, J. Y., & Lin, Z. C. (2014). Paleo-CO_2 variation trends and the Cretaceous greenhouse climate. *Earth-Science Reviews, 129*, 136–147. http://dx.doi.org/10.1016/j.earscirev.2013.11.001.

Wang, P. J., Liu, W. Z., Wang, S. X., & Song, W. H. (2002). $^{40}Ar/^{39}Ar$ and K/Ar dating on the volcanic rocks in the Songliao basin, NE China: constraints on stratigraphy and basin dynamics. *International Journal of Earth Sciences, 91*, 331–340. http://dx.doi.org/10.1007/s005310100219.

Wang, P. J., Ren, Y. G., Shan, X. L., Sun, S. B., Wan, C. B., & Bian, W. H. (2002). The Cretaceous volcanic succession around the Songliao Basin, NE China: relationship between volcanism and sedimentation. *Geological Journal, 37*, 97–115. http://dx.doi.org/10.1002/gj.905.

Wang, P. J., Xie, X. A., Frank, M., Ren, Y. G., Zhu, D. F., & Sun, X. M. (2007). The Cretaceous Songliao Basin: volcanogenic succession, sedimentary sequence and tectonic evolution, NE China. *Acta Geologica Sinica (English Edition), 81*, 1002–1011. http://dx.doi.org/10.1111/j.1755-6724.2007.tb01022.x.

Wang, P. J., Zhao, R. L., Meng, Q. A., Que, X. J., Zhu, D. F., & Gao, Y. F. (2015). The Cretaceous Songliao Basin: dynamic background from volcanic rift to interior sag basin. *Earth Science Frontiers, 22*, 72–91 (in Chinese with English abstract).

Wignall, P. B. (2001). Large igneous provinces and mass extinctions. *Earth-Science Reviews, 53*, 1–33. http://dx.doi.org/10.1016/S0012-8252(00)00037-4.

Williams, I. (1998). U-Th-Pb geochronology by ion microprobe. In M. A. McKibben, W. C. Shanks, III, & W. I. Ridley (Eds.), *Applications of microanalytical techniques to understanding mineralizing processes, reviews in economic geology* (Vol. 7, pp. 1–35).

Wu, Q., Pu, R. H., Han, M. Q., Cao, H. H., & Li, Q. (2010). Zircon LA-ICP-MS U-Pb dating for the volcanic rocks in Changling depression, and its geological implication. *Journal of Mineralogy and Petrology, 30*, 111–119 (in Chinese with English abstract).

Xiao, J., Chen, H. L., Yang, S. F., Zhang, F. Q., Lin, X. B., Yu, X., et al. (2011). Gas charging of deep volcanic reservoirs in the northern Songliao Basin: evidence from fluid inclusion. *Acta Petrolei Sinica, 32*, 968–975 (in Chinese with English abstract).

Young, S. A., Saltzman, M. R., Foland, K. A., Linder, J. S., & Kump, L. R. (2009). A major drop in seawater $^{87}Sr/^{86}Sr$ during the Middle Ordovician (Darriwilian): links to volcanism and climate? *Geology, 37*, 951–954. http://dx.doi.org/10.1130/G30152A.1.

Yuan, H. L., Gao, S., Liu, X. M., Li, H. M., Gunther, D., & Wu, F. Y. (2004). Accurate U–Pb age and trace element determinations of zircon by laser ablation-inductively coupled plasma mass spectrometry. *Geostandard Newsletters, 28*, 353–370. http://dx.doi.org/10.1111/j.1751-908X.2004.tb00755.x.

Zakharov, Y. D., Baraboshkin, E. Y., Weissert, H., Michailova, I. A., Smyshlyaeva, O. P., & Safronov, P. P. (2013). Late Barremian-early Aptian climate of the northern middle latitudes: stable isotope evidence from bivalve and cephalopod molluscs of the Russian platform. *Cretaceous Research, 44*, 183–201. http://dx.doi.org/10.1016/j.cretres.2013.04.007.

Zhang, F. Q., Chen, H. L., Dong, C. W., Pang, Y. M., Shu, P., Wang, Y. L., et al. (2008). Shrimp zircon U-Pb geochronology of volcanic rocks and discussion on the geological time of the Yingcheng Formation of the northern Songliao Basin. *Journal of Stratigraphy, 32*, 15–20 (in Chinese with English abstract).

Zhang, F. Q., Cheng, X. G., Chen, H. L., Dong, C. W., Yu, X., Xiao, J., et al. (2009). Ziron chronological and geochemical constraints on the Late Mesozoic volcanic events in the southeastern margin of the Songliao Basin, NE China. *Acta Petrologica Sinica, 25*, 39–54 (in Chinese with English abstract).

Zhang, F. Q., Chen, H. L., Yu, X., Dong, C. W., Yang, S. F., Pang, Y. M., et al. (2011). Early Cretaceous volcanism in the northern Songliao Basin, NE China, and its geodynamic implication. *Gondwana Research, 19*, 163–176. http://dx.doi.org/10.1016/j.gr.2010.03.011.

Zhang, J. H., Ge, W. C., Wu, F. Y., Wilde, S. A., Yang, J. H., & Liu, X. M. (2008). Large-scale Early Cretaceous volcanic events in the northern Great Xing'an Range, northeastern China. *Lithos, 102*, 138–157. http://dx.doi.org/10.1016/j.lithos.2007.08.011.

Zhang, F. Q., Pang, Y. M., Yang, S. F., Dong, W. C., Chen, H. L., & Shu, P. (2007). Geochronology of zircon SHRIMP, geochemistry and its implication of the volcanic rocks from Yingcheng Formation in depression area, north of Songliao Basin. *Acta Geologica Sinica, 81*, 1248–1258 (in Chinese with English abstract).

Zielinski, G. A. (2000). Use of paleo-records in determining variability within the volcanism-climate system. *Quaternary Science Reviews, 19*, 417–438. http://dx.doi.org/10.1016/S0277-3791(99)00073-6.

Zielinski, G. A., Mayewski, P. A., Meeker, L. D., Whitlow, S., Twickler, M. S., Morrison, M., et al. (1994). Record of volcanism since 7000 B.C. From the GISP2 Greenland ice core and implications for the volcano-climate system. *Science, 264*, 948–952.